Numerical Weather Prediction activities at CHMI

Czech Hydrometeorological Institute

R. Brožková, A. Bučánek, J. Mašek, D. Němec, A. Šljivić , P. Smolíková, A. Trojáková

NWP system

ALADIN/CHMI couples non-hydrostatic (NH) dynamics and the set of ALARO-1vB physical parameterizations suited for modeling of atmospheric motions from planetary up to the meso-gamma scales:

- domain 1069x853 grid points, Δx~2.3km
- linear truncation E539x431
- 87 vertical levels, mean orography
- ICI scheme with 1 iteration, time step 90 s
- 3h coupling interval
- 00, 06, 12/18 UTC forecast to +72/54h
- hourly analysis system VarCan Pack
- ALADIN cycle 46t1mp (ALARO-1vB)

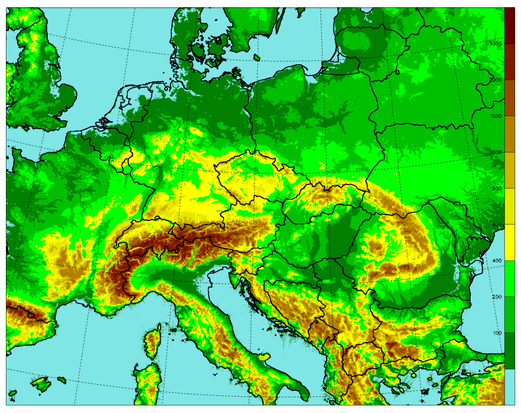

Fig. 1. *Orography of the domain.*

Data assimilation includes surface analysis based on an optimal interpolation (OI) and BlendVar analysis for upper air fields, which consists of the digital filter spectral blending (Brozkova et al.,2001) followed by the 3DVAR analysis (Fischer et al., 2005)

- digital filtering at truncation E102x81; space consistent coupling
- no DFI in long cut-off 3h cycle; incremental DFI in short cut-off production analysis
- observations: SYNOP, TEMP, AMDAR, Mode-S, SEVIRI, WP, HR-AMV, ASCAT

HPC systems

Two HPC systems at CHMI:

NEC SX Aurora TSUBASA
48 computing nodes with:
- one **AMD EPYC** 7402 CPU (24 cores, 512GB RAM) , and
- eight **NEC Vector Engines** 20B (8 cores, 48GB RAM each)

- total **1152 VH + 3072 VE cores**

NEC LX series HPC cluster
- 320 computing nodes with:
- **Intel Broadwell** CPU (2x12 cores, 64GB RAM)
- total **7680 computational cores**

Fig. 2. *NEC SX Aurora*

New convective diagnostics

A set of convective diagnostics was implemented in cooperation with the CHMI convection-specialized team and became operational in May 2023. Firstly, selected already available visualizations were revised, for example the visualization of CAPE was enhanced for CIN and moisture convergence (Figure 3) or alternatively for wind shear between the low level and a mid-tropospheric level (Figure 4), Secondly, new products, including storm relative helicity (Figure 5), updraft and downdraft track, and updraft helicity track (Figure 6) were added. These new products are useful for determining the type of convective storm, e.g. squall lines or supercells; eventually for predicting favorable environment for tornado development.

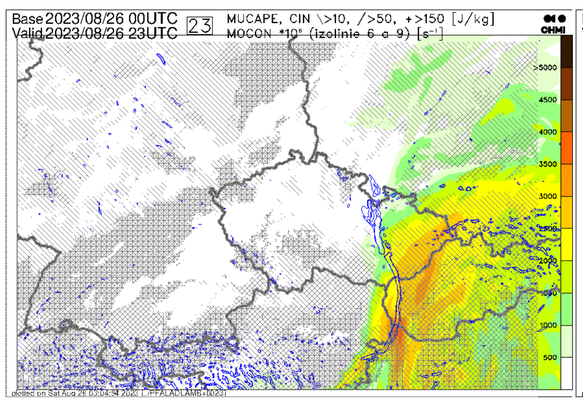

Fig. 3. *Combination of Most Unstable CAPE (colors), CIN (hatching) and moisture convergence near the ground (isoline) for 26 Aug 2023 00UTC +23h.*

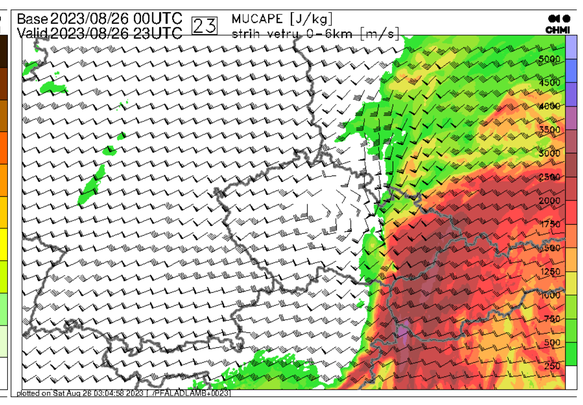

Fig. 4. *Combination of Most Unstable CAPE (colors) and wind shear (wind arrows) between the near surface and 6km for 26 Aug 2023 00UTC +23h.*

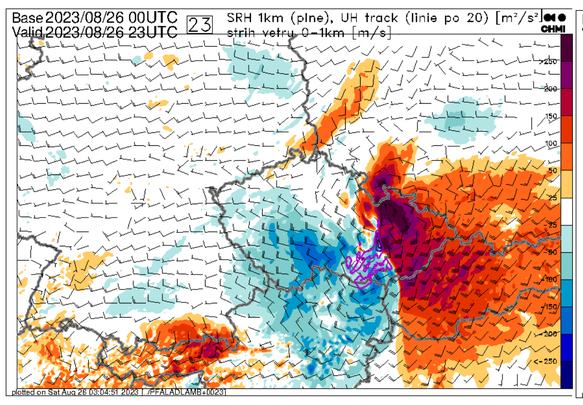

Fig. 5. *Combination of Storm Relative Helicity (colors), Updraft Helicity track (isoline) and wind shear (wind arrows) between the near surface and 1km.*

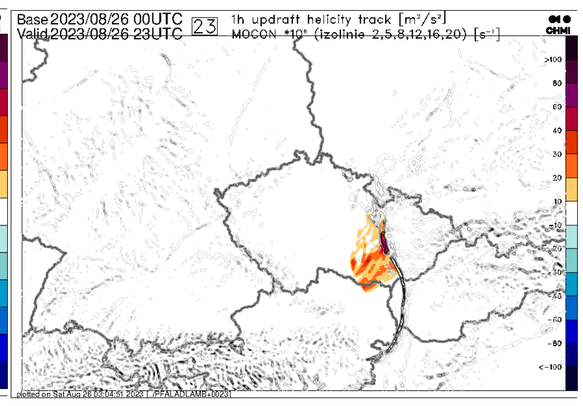

Fig. 6. *Combination of Updraft Helicity track (colors) and moisture convergence (isoline) for 26 Aug 2023 00UTC + 23h.*

Major operational changes

15 May 2023	New convective diagnostics (see description in the left panel)
6 Feb 2024	Increase of long cut-off assimilation frequency to 3h and the new setting of surface assimilation and snow roughness (see description below). The new Lopez evaporation parametrization and retuned autoconversions to snow and cloud water (presentation of David Němec).

New snow treatment

The original surface analysis setup included a weak relaxation to the climatology (RCLIMCA=0.045). We halved it (RCLIMCA=0.0225) when switching to a 3-hour cycle (complete removal of relaxation caused a bias of 2m temperature and a small daily amplitude). However, we left it off for snow to get more realistic amount of snow.

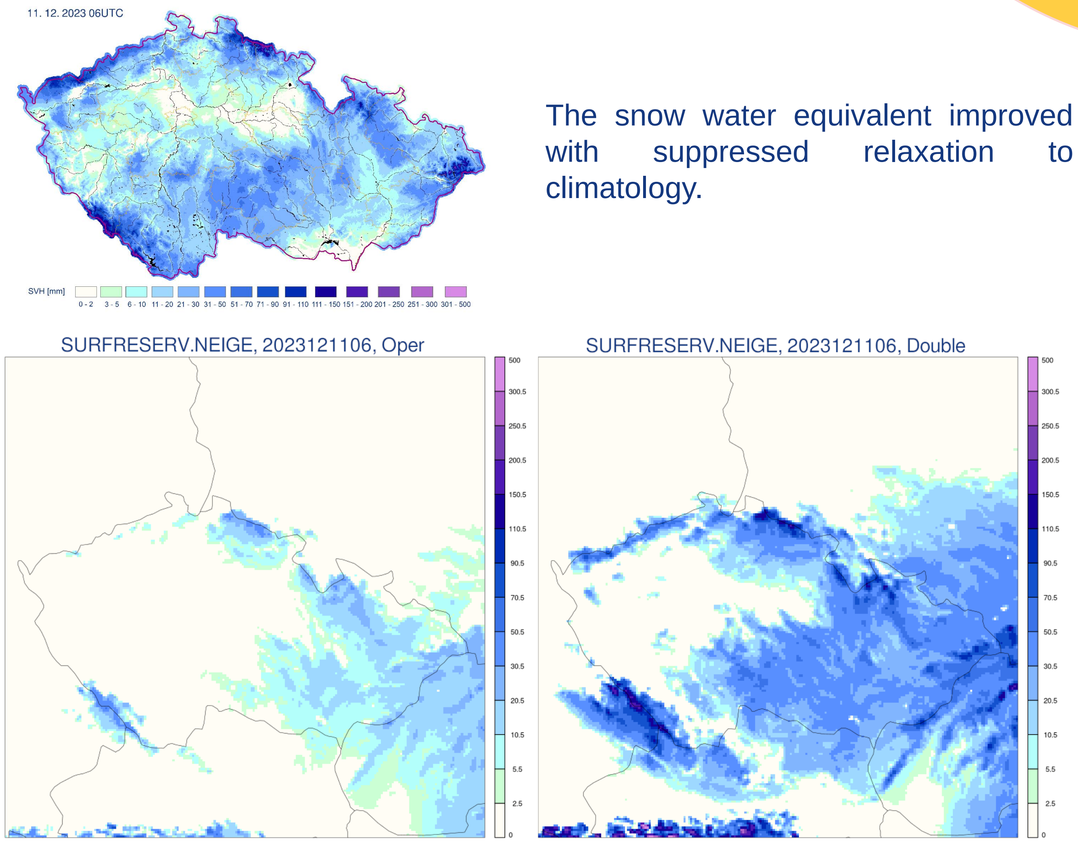

Fig. 7. *Snow water equivalent (SWE) for 11 Dec 2023 06UTC, OPER (left) with a weak relaxation (RCLIMCA=0.045) and parallel test (right) with suppressed relaxation for snow (RCLIMSN=0) and the observation based estimate of SWE (top).*

The snow water equivalent improved with suppressed relaxation to climatology.

Larger amounts of snow needed adjustments to the roughness of the vegetation covered by snow (effect on wind speed) and its distribution within the grid-box (effect on temperature due to radiation).

The old treatment was averaging roughness lengths of vegetation and snow using snow fraction as weight. In case of large amount of snow over forest, it led to unrealistic reduction of roughness length, resulting in overestimated 10m wind speed. The new treatment employs approximate relation between mean obstacle height and roughness length, and it reduces the roughness length proportionally to the part of obstacle height covered by snow.

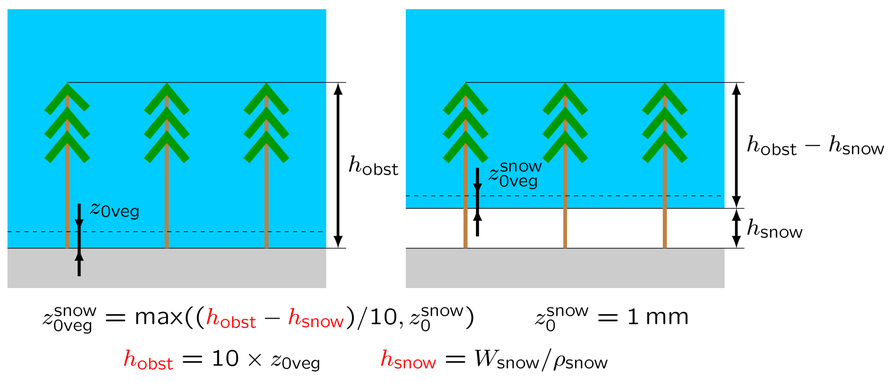

The new treatment (LZ0SNOWH=T, RZ0_TO_HEIGHT=0.1) was introduced (available since CY49T1) improving the bias of 10m wind speed (Figure 8). Cold bias of 2m temperature connected to higher amount of snow was reduced by retuning the snow fraction (parameter WCRIN is set to 10 instead of 4).

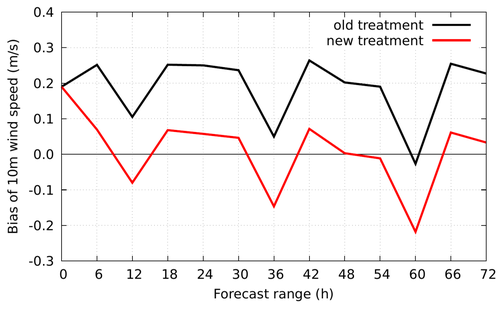

Fig. 8. *Time evolution of BIAS of 10m wind speed for period of 1 – 8 Dec 2023 00UTC. Reference (old treatment) and new treatment of* roughness lengths.

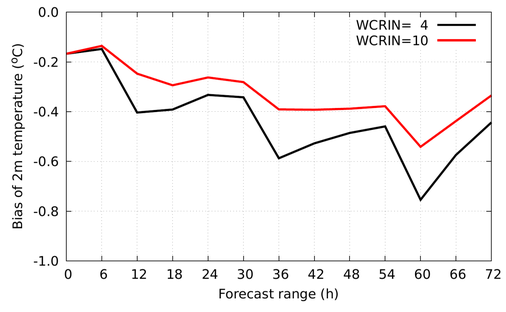

Fig. 9. *Time evolution of BIAS of 2m temperature for period of 1 – 8 Dec 2023 00UTC. Reference (WCRIN=4) and new setting (WCRIN=10).*